

Accepted Manuscript

Assessment of the thermomechanical performance of continuous glass fiber-reinforced thermoplastic laminates

M. Nikforooz, J. Montesano, M. Golzar, M.M. Shokrieh

PII: S0142-9418(18)30029-1

DOI: [10.1016/j.polymertesting.2018.02.023](https://doi.org/10.1016/j.polymertesting.2018.02.023)

Reference: POTE 5347

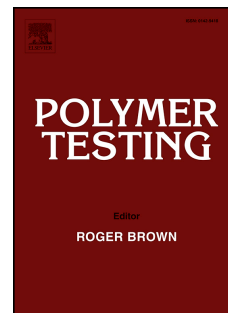
To appear in: *Polymer Testing*

Received Date: 7 January 2018

Accepted Date: 20 February 2018

Please cite this article as: M. Nikforooz, J. Montesano, M. Golzar, M.M. Shokrieh, Assessment of the thermomechanical performance of continuous glass fiber-reinforced thermoplastic laminates, *Polymer Testing* (2018), doi: [10.1016/j.polymertesting.2018.02.023](https://doi.org/10.1016/j.polymertesting.2018.02.023).

This is a PDF file of an unedited manuscript that has been accepted for publication. As a service to our customers we are providing this early version of the manuscript. The manuscript will undergo copyediting, typesetting, and review of the resulting proof before it is published in its final form. Please note that during the production process errors may be discovered which could affect the content, and all legal disclaimers that apply to the journal pertain.



Material Properties

Assessment of the thermomechanical performance of continuous glass fiber-reinforced thermoplastic laminates

Nikforooz, M¹, Montesano, J³, Golzar, M^{1*}, Shokrieh, MM²,

¹ Department of Mechanical Engineering, Tarbiat Modares University, Jalaale-al Ahmad Ave., P.O. Box 14115-143, Tehran, Iran

² Composite Research Laboratory, Center of Excellence in Experimental Solid Mechanics and Dynamics, School of Mechanical Engineering, Iran University of Science and Technology (IUST), Narmak, 16846-13114 Tehran, Iran

³ Department of Mechanical & Mechatronics Engineering, University of Waterloo, 200 University Ave. West, Waterloo, Canada N2L3G1

* Corresponding author (m.golzar@modares.ac.ir; Tel. +98-21-82884320)

Abstract

The effects of temperature on the static tensile behavior of continuous E-glass/polyamide laminates were studied in order to assess the feasibility of using the material system for structural applications. Uniaxial tensile tests were conducted on $[0]_8$, $[90]_8$, $[0_2/90_2]_s$ and $[0_4/90_4]_s$ laminates at multiple temperatures above and below the glass transition temperature, which was measured using different methods. Optical and scanning electron microscopy were performed on the tested samples, and the effects of temperature on failure modes were investigated. The $[0]_8$ and $[90]_8$ laminates displayed three reduction stages in modulus versus temperature, where the largest reduction was in the glass transition region as a result of notable softening of the polyamide matrix, as confirmed by fractographic analysis. However, the $[0_2/90_2]_s$ and $[0_4/90_4]_s$ laminates displayed the largest modulus reduction prior to the glass transition temperature with little reduction beyond, which was attributed to matrix softening coupled with in situ ply constraining effects.

Keywords: (Thermomechanical behavior; Continuous glass/polyamide; Fractography; Mechanical properties)

1. Introduction

Continuous fiber-reinforced thermoplastic composites possess high toughness and recyclability and, therefore, are gaining more attention in industry as an alternative to more conventional thermosetting composites for primary structural applications. Nonetheless, a number of barriers must be overcome before usage of these thermoplastic-based composites becomes widespread. For example, processing continuous fiber-reinforced thermoplastics is challenging compared to their thermosetting counterparts due to the higher processing temperatures required and higher melt viscosity. Also, some thermoplastics such as polyamide are susceptible to extreme environmental conditions due to their relatively low glass transition temperatures [1]. Under these conditions, not only are the mechanical properties notably reduced due to the softening of the matrix, but the fiber/matrix interface integrity is also weakened by temperature rise due to induced thermal stresses caused by thermal expansion coefficient mismatch of the constituents. Therefore, improved understanding of the thermomechanical performance of continuous fiber-reinforced thermoplastics is required.

A number of studies focused on assessing the influence of fiber and matrix type as well as fiber architecture on the performance of fiber-reinforced thermoplastic composites have been reported during the past two decades. Huang et al. [2] investigated the effect of temperature on two cross ply laminates with the same fiber type, namely graphite/bismaleimide (thermoset) and graphite/Avimid (thermoplastic). They concluded that the fracture toughness was higher for the thermoplastic composite, which for both material systems decreased with temperature. Vieille et al. [3] examined the mechanical behavior of quasi-isotropic woven carbon/epoxy and carbon/PPS composites at 120 °C, and concluded that the ductility of carbon/PPS limited the notch stress concentrations at this temperature. Sorrentino et al. [4] studied the effect of temperature on flexural and low velocity impact behavior of four thermoplastic PEN-based composites with carbon, Tawaron, Vecteran and basalt fibers, and found that basalt/PEN has the best impact performance compared to the other three composites. Celestine et al. [5] investigated the effect of temperature on the mechanical properties of carbon/polyamide composites with different fiber architectures, including discontinuous, unidirectional and woven composites, and concluded that

temperature has less effect on mechanical properties of aligned fibers. With respect to fiber length, Rezaei et al. [6] studied the effect of carbon fiber length on the thermomechanical behavior and thermal stability of short carbon/PP composites via thermal gravimetric analysis (TGA), and concluded that increasing fiber length increased the thermal stability of the composite. In contrast to the aforementioned studies, Valentin et al. [7] studied the effect of temperature on the mechanical behavior of pure polyamide, short glass fiber-reinforced and continuous fiber-reinforced polyamide composites between $-40\text{ }^{\circ}\text{C}$ and $140\text{ }^{\circ}\text{C}$. They found the effect of temperature more influential on stress at rupture for continuous composites.

In addition, a number of recently reported studies reveal that temperature has distinct influence on different mechanical properties [8–12]. For example, Gabrion et al. [8] studied the stability and thermomechanical behavior of unidirectional thermoplastic carbon/polyimide composites. They observed retention of the tensile and shear mechanical properties until $200\text{ }^{\circ}\text{C}$, except for the interfacial shear strength. Gibson et al. [9] investigated the high temperature behavior of thick woven glass/PP composites under tensile and compressive loading and found that, at high temperatures, mechanical properties under compression degraded more severely compared to tensile loading. A number of studies have also expressed the dependency of Young's modulus and strength on temperature in mathematical formulations. For example, Reis et al. [10] studied the effect of temperature and strain rate on the behavior of woven glass/epoxy composites and found the effect of temperature more influential on Young's modulus than strength. Alcock et al. [11] investigated the effect of temperature on the strength and Young's modulus of all-PP composites, where a master curve was developed and Arrhenius relations were used to extrapolate strength and Young's modulus data for different temperatures. Hufenbach et al. [12] examined the temperature effect on the mechanical properties of 3-D textile-reinforced and woven glass/PP composites. They investigated damage growth and void growth at different temperatures for both tensile and compressive loading from $-40\text{ }^{\circ}\text{C}$ to $80\text{ }^{\circ}\text{C}$.

Recently, polyamide 6 has attracted attention as a potential alternative to thermosets for structural composite materials [13]. Although low-cost polyamide composites possess some key advantages, the

main drawback of this material is its low glass transition temperature which may limit its applicability [14]. Some studies have investigated the thermomechanical behavior of glass/polyamide composites, most of which are limited to short fiber composites [15–16]. Launay et al. [15] investigated the effect of temperature and humidity on the mechanical behavior of short glass fiber-reinforced polyamide composites and suggested a law which considers the effects of humidity and temperature on the material behavior to be equivalent. Wang et al. [16] studied the effect of temperature and strain rate on the tensile behavior of short E-glass/polyamide composites both in the extrusion direction and perpendicular to the extrusion direction. They established a strain rate and temperature-dependent model for the behavior of the material in both directions. Eftekhari and Fatemi [17] examined the behavior of different short glass fiber-reinforced thermoplastic composites including glass/polyamide 6.6 under different environmental conditions and different temperatures. They found a bi-linear reduction for strength and stiffness of glass/Pa 6.6 at temperature range including glass transition temperature.

Continuous E-glass/polyamide is considered a potential cost-effective substitute for high performance thermoset composites such as E-glass/epoxy in wind turbine blades [18]. For these applications the material can be exposed to different temperatures near or above the glass transition temperature, thus a deeper understanding of the thermomechanical performance is required in order to account for potential reductions in its structural integrity. There are a few studies focused on assessing the effect of temperature on the mechanical behavior of continuous E-glass/polyamide composite laminates [5,19-23]. Pegoretti et al. [19,20] studied the interfacial fracture toughness and also interfacial shear strength of glass/nylon microcomposites with different sizing of fiber surface at different temperatures and concluded that increasing temperature decreases the interfacial toughness and interfacial shear strength noticeably. Recently, Machado et al. [21] investigated the thermomechanical behavior of woven carbon/polyamide and glass/polyamide composites using dynamic mechanical thermal analysis (DMTA) in tensile mode and modeled the material's viscoelastic behavior with Prony series. Similarly, Ropers et al. [22] used dynamic mechanical analysis (DMA) and rheometry in bending mode instead of conventional mechanical tests at different temperatures to study the bending stiffness of woven glass/polyamide and unidirectional

carbon/polyamide composites versus temperatures. They used linear Prony series and also a non-linear model to express the viscoelastic behavior of the material.

Although the work reported in the cited literature has significantly advanced the knowledge base for thermoplastic composites, there is a lack of experimental data and fundamental understanding of the effect of temperature on the performance of continuous glass/polyamide laminates, in particular their tensile mechanical properties. Therefore, the focus of the current study is to assess the mechanical properties of cost-effective continuous E-glass/polyamide laminates at various ambient temperatures, at both the lamina and laminate level. One of the main goals is to better understand the underlying mechanisms influencing the mechanical performance under quasi-static loading conditions.

2 Material and Experimental Details

It should be mentioned that all the experimental tests in this paper were performed at the University of Waterloo.

2.1 Laminate Processing

E-glass/polyamide prepreg from Jonam Ltd. was used for the fabrication of $[0]_8$, $[90]_8$, $[0_2/90_2]_s$ and $[0_4/90_4]_s$ laminates. A 30-ton Carver hot press was used for fabrication of the panels with a maximum processing temperature of 240 °C and consolidation pressure of 0.9 bar. The resulting fiber volume fraction for the fabricated composites was approximately 58%, with high quality and minimal void formations [23].

2.2 Glass Transition Temperature Determination

The glass transition temperature (T_g) of the material was determined using three different methods, namely differential scanning calorimetry (DSC), dynamic mechanical analysis (DMA) and thermomechanical analysis (TMA).

DSC was carried out using a Netzsch DSC 200 F3 Maia® under a nitrogen atmosphere to prevent material oxidation. A mass of 7.539 mg of E-glass/polyamide prepreg was sealed in an aluminum pan. The material was heated from 25 °C to 350 °C at a rate of 10 °C/min.

DMA was performed on $[0_2/90_2]_s$ laminates using a TA Instruments DMA Q800 according to ASTM D4092. The dimensions of the specimens were 47 mm x 1.52 mm x 1.3 mm. The frequency of the tests and the heating rate were set at 2 Hz and 2 °C/min, respectively.

TMA tests were performed on $[0_2/90_2]_s$ specimens in compression mode using a TA Instruments Q400. The dimensions of the specimens were 9 mm x 9 mm x 1.47 mm. The temperature of the specimen was increased from room temperature to 110 °C at a rate of 1 °C/min.

2.3 Mechanical Tensile Tests at Different Temperatures

Tensile tests were performed on $[0]_8$ and $[90]_8$ specimens at 23 °C, 50 °C, 80 °C and 100 °C, and on $[0_2/90_2]_s$ and $[0_4/90_4]$ at the same temperatures as well as at 40 °C, using an MTS Criterion® Model 45 with a custom MTS environmental chamber at a displacement rate of 2 mm/min. Digital image correlation (DIC) was used for capturing strain fields in the specimens during loading. Straight-sided specimens were prepared for the tests based on ASTM D3039, and aluminum alloy end tabs were bonded on both ends of the specimens. The geometry of the specimens and the dimensions are shown in Figure 1 and Table 1.

2.4 Scanning and optical electron microscopy of fractured samples

Scanning electron microscopy (SEM) of fracture surfaces was carried out using a Zeiss Leo 1530 microscope. Furthermore, optical microscopy was performed on mounted fractured samples using an Olympus microscope equipped with a 5 MP camera. Samples with 22 mm length-wise section were cut from the middle of the specimens which were tested at 23 °C, 50 °C, 80 °C and 100 °C. The sections were mounted and polished with sandpapers of 6 different grit sizes and also four different grades of alumina powder suspension.

3. Results and discussion

3.1 Glass transition temperature comparison

Figure 2 presents the DSC thermogram for E-glass/polyamide. It shows a maximum peak temperature of 230 °C which corresponds to the melting temperature of the matrix. There are two inflection points representing possible glass transition temperatures at 42.8 °C and 75.8 °C, which can be referred to as the wet and dry T_g respectively. This is corroborated by Ref. [24] which states that humidity can decrease the glass transition temperature noticeably.

From the DMA test, the storage modulus (E'), loss modulus (E'') and $\tan(\delta)$ versus temperature curves are presented in Figure 3. The glass transition temperature can be interpreted as the inflection point in storage modulus, the peak point in $\tan(\delta)$ or loss modulus, the latter being the ASTM D4065 recommendation. Based on the peak in loss modulus and $\tan(\delta)$, the glass transition temperature is 63 °C and 67 °C, respectively.

From the TMA test as seen in Figure 4, the inflection point is nearly 61.7 °C, which represents the glass transition temperature of the material.

Results from the three methods presented produced a range of possible T_g values. Previous reported studies generally accept glass transition temperature results evaluated from DMA as the most accurate, thus the T_g for the E-glass/polyamide composite is reported in the range of 63–67 °C. Note that this value is similar to the value extracted using TMA tests.

3.2 Unidirectional laminate tensile tests

3.2.1 $[0]_8$ Laminates

Figure 5 presents tensile strength and tensile modulus versus temperature for $[0]_8$ specimens. Figure 5(a) shows that the tensile strength decreases with increasing temperature, particularly between 50 °C and 100 °C. In this temperature range, two competing mechanisms contribute to the behavior observed. First, the polyamide amorphous phase transitions from a solid state to a rubbery state and, second, the bonding between the fiber and the matrix is weakened as the ambient temperature increases. The result of the

former mechanism is shear failure of the polyamide matrix, as supported by a thin layer of polyamide matrix observed on the surface of the fibers. For the latter mechanism, bare fibers can be observed after specimen failure which confirms the weak interface between the fibers and the matrix. These findings are supported by SEM images of the fracture surfaces, shown in Figure 6 for $[0]_8$ specimens at 23 °C, 50 °C and 80 °C. In the $[0]_8$ laminate, brittle matrix fracture is observed in specimens tested at 23 °C, while plastic flow of the polyamide matrix and also more bare fibers are observed in specimens tested at 50 °C and 80 °C. In these cases, the matrix is malleable so the fracture is ductile and the weakened interface between the fiber and the matrix causes more splitting cracks in longitudinal layers.

Figure 5(b) shows that the Young's modulus does not change between room temperature and 50 °C. The insensitivity of the specimens' stiffness within this range is due to the fact that both glass fibers and polyamide are in a rigid state. As the temperature increases from 50 °C to 80 °C, the Young's modulus decreases by 16.4 %. Based on this sudden change in the Young's modulus near the measured glass transition temperature (i.e., 63–67 °C), this behaviour can be attributed to the transition of the amorphous phase of the semi-crystalline matrix from a rigid to a rubbery state. Between 80 °C to 100 °C, the Young's modulus did not change significantly. Beyond the glass transition temperature, the amorphous phase of the thermoplastic matrix continues to soften but the crystalline phase is still rigid, and any further increase in temperature only increases the mobility of polyamide chains in the amorphous phase. Furthermore, fiber-dominated behavior of $[0]_8$ laminates prevents further decrease in Young's modulus between 80 °C to 100 °C.

The rule of mixtures (ROM) was used to evaluate the Young's modulus at different temperatures using the matrix modulus corresponding to a particular temperature. As seen in Figure 5(b), the rule of mixtures can predict the upper bound of the Young's modulus at room temperature very well, however this rule does not produce accurate predictions for Young's modulus at higher temperatures and only indicates that a drop occurs in the glass transition region. This is due to the assumption of perfect bonding

in the rule of mixtures which is not true for thermoplastic composites at temperatures higher than room temperature [25,26].

Figure 7 presents the representative stress-strain curves for $[0]_8$ laminates tested at different temperatures. As seen in the figure, the strain to failure decreases as the temperature increases. The reason is that, as temperature increases, the bonding between the fibers and the matrix weakens and glass/polyamide interfacial toughness reduces, as was mentioned in Ref. [19], causing the number of splitting failure cracks to increase in spite of increased plasticity in the matrix. Furthermore, fibers in splitting sections bear more load causing them to break sooner. As seen in Figure 7(b), the number of splitting cracks increase drastically between 80 °C and 100 °C.

3.2.2 $[90]_8$ Laminates

Figure 8(a) presents the tensile strength versus temperature for neat polyamide [27] and glass/polyamide $[90]_8$ specimens. It is shown that polyamide's strength decreases drastically between 40 °C and 80 °C and more gradually thereafter. However, in glass/polyamide $[90]_8$ specimens, the trend is different as the curve shows a more gradual decrease between 40 °C and 80 °C, with the rate of this decrease increased between 80 °C and 100 °C. This behavior was also observed for longitudinal specimens within this temperature range, and can be attributed to weakening of the fiber-matrix interface bond with increasing temperature as well as softening of the matrix and corresponding plastic deformation at 100 °C. Figure 9 presents the SEM images for failed $[90]_8$ specimens at 23 °C, 50 °C, 80 °C and 100 °C. As seen in the figure, debonding occurs at 23 °C, 50 °C and 80 °C but, at 100 °C, large plastic deformation of the polyamide matrix is observed around the fibers. These observations again validate the 17.2% and 40.4% strength reductions at 80 °C and 100 °C, respectively, compared to that observed at 23 °C.

As seen in Figure 8(b), as temperature approaches 50 °C there is a 10% decrease in experimental Young's modulus. This reduction can be explained by the matrix dominance of this lamination, such that any increase in temperature would increase molecular mobility. From 50 °C to 80 °C there is a sudden

large decrease of 17.4 % in Young's modulus which again supports the measured glass transition temperature between 63 °C and 67 °C. Finally from 80 °C to 100 °C, there is 4.2 % decrease in the Young's modulus. In this temperature range, the amorphous phase of the matrix has been completely softened and any further increase in temperature would only increase the mobility of molecules in the amorphous phase. It is clear that the overall temperature dependence of the laminate modulus is analogous to that observed for the polyamide matrix (see Fig. 8(b)).

The rule of mixtures was used for the prediction of the transverse Young's modulus at different temperatures. As seen in Figure 8(b), the Young's modulus is 24 % lower in experiments than obtained by the rule of mixtures. This large difference can be because of the high Young's modulus of polyamide in [27] which is in the upper bound of the available data for polyamide Young's modulus in the literature. Another reason for this difference can be the weak bonding between the fibers and polyamide matrix so that the matrix cannot transfer the load to the fibers.

As seen in Figure 10(a), the strain to failure increases between 23 °C and 80 °C as a result of matrix softening, but it decreases between 80 °C and 100 °C. At 100 °C, the matrix has a large plastic deformation and, in contrast to the other three temperatures, there is no sudden drop in the stress-strain curve. Instead, there is a gradual decrease in this curve after the ultimate strength point which is due to necking of the polyamide matrix. As seen in Figure 10(b), there is a large plastic deformation in polyamide matrix at this temperature that is shown by the fiber bridging between the two parts of the failed specimen. In fact, there are two competing failure mechanisms in transverse loading termed fiber-matrix debonding and ductile failure of the matrix [28] in which the former occurs at 23 °C, 50 °C and 80 °C and the latter occurs at 100 °C.

3.3 Cross-ply laminate tensile tests

3.3.1 [0₂/90₂]_s Laminates

Figure 11(a) presents the tensile strength versus temperature for [0₂/90₂]_s specimens. The figure shows a slight decrease from 23 °C to 40 °C, a 25 % decrease between 40 °C and 80 °C and, finally, a

slight increase in strength between 80 °C and 100 °C. The conclusion is that the maximum decrease in the strength is below the glass transition temperature.

It should be noted that this behaviour is in contrast to that observed with the $[0]_8$ and $[90]_8$ specimens. Degradation of the laminate strength at increasing ambient temperatures can be attributed to degradation of the transverse ply strength up to 80 °C and, since the central transverse layer is thicker than the individual on-axis layers, the effect on the laminate is more pronounced. Beyond 80 °C, plastic deformation of the matrix in the transverse layers is more severe and, although the on-axis layers exhibit local matrix plastic deformation, the constraining effect of these layers on the transverse layers limits any further degradation of the laminate strength. This constraining effect imparted by the on-axis plies may also act to mitigate crack initiation in the 90 layers at 100 °C. This result is quite remarkable from a design perspective since, for a laminate, the strength degradation at temperatures greater than T_g , can be mitigated for the E-glass/polyamide cross-ply laminate.

Fractography provides insight to better understand the behavior of the material at the tested temperatures in Figure 12. SEM images of the failed $[0_2/90_2]_s$ specimens show that at room temperature the behavior of the polyamide matrix is brittle and chunks of polyamide matrix are adhered to the fiber surface. At 40 °C, SEM images show generally brittle fracture, although plastic deformation of the polyamide matrix is observed locally at the tips of some fractured fibers and also in some debonded areas (see figure 12(b)). At these stress concentration areas, an increase of 15 °C above room temperature causes local plastic deformation of the polyamide matrix, primarily observed in the matrix-dominated 90° plies. At 50 °C, plastic deformation of the polyamide matrix is widely observed in the transverse layer, and, at 80 °C, large plastic deformation of the matrix is seen both in longitudinal and transverse layers. As with the other laminates, these images again corroborate the strength reductions that were observed at 50 °C and 80 °C.

To understand the effect of temperature on the material's stiffness, the Young's modulus of $[0_2/90_2]_s$ specimens have been plotted versus temperature in Figure 11(b). As temperature increases from 23 °C to

40 °C, a noticeable decrease of 17.1 % occurs in the Young's modulus. However, between 40 °C to 50 °C this reduction is only 6.3 %, and there is nearly no change between 50 °C to 100 °C. Modulus degradation of the laminate up to 50 °C can be attributed to modulus degradation and inelastic deformation of the transverse layer due to local matrix softening, while no degradation is exhibited beyond this temperature since the constraining effects from the on-axis plies become more prominent. Classical lamination theory (CLT) was used to obtain Young's modulus versus temperature for $[0_2/90_2]_s$ specimens. As seen in Figure 11(b), CLT can accurately predict Young's modulus at room temperature and above the glass transition temperature (i.e. 80 °C and 100 °C), but it is inaccurate between 40 °C and 50 °C due to the modulus degradation and inelastic behaviour of the transverse layer. Using CLT again and ignoring the stiffness of 90 degree layers, the laminate stiffness is nearly the same as is obtained experimentally at these temperatures. This implies that the 90 degree layers are not fully effective at these temperatures. This discussion will be expanded in the next section for $[0_4/90_4]_s$ laminates.

The representative stress-strain curves for $[0_2/90_2]_s$ specimens tested at different temperatures are shown in Figure 13(a). As seen in Figure 13(a), the strain to failure decreases as the temperature increases between 23 °C and 80 °C as a result of strength degradation of the transverse layer, however, it is constant beyond 80 °C. As seen in Figure 13(b), the failure is brittle and localized especially at 23 °C, 50 °C and 80 °C, however it is more ductile at 100 °C with drastically more splitting cracks at this temperature.

3.3.2 $[0_4/90_4]_s$ Laminates

Figure 14(a) presents the tensile strength versus temperature for $[0_4/90_4]_s$ specimens. Between 23 °C and 40 °C and between 40 °C to 50 °C there is, respectively, 10 % and 16.8 % decrease in tensile strength, although the strength is nearly constant between 50 °C and 100 °C. These significant results are analogous to those observed for the $[0_2/90_2]_s$ laminates where degradation of the transverse layer strength up to 50 °C causes degradation of the laminate strength, beyond which constraining effects imparted by the on-axis plies mitigates any further laminate strength degradation. It should be noted that, for the

thicker cross-ply laminate, the influence of this constraining effect was observed starting at 50 °C, while for the thinner cross-ply laminate starting at 80 °C (compare Figures 11 and 14).

Furthermore, by comparing the strength versus temperature for $[0_2/90_2]_s$ and $[0_4/90_4]_s$ laminates, it is evident that the strength in $[0_4/90_4]_s$ is lower than its corresponding value at the same testing temperature in $[0_2/90_2]_s$ laminates. To better explain this behaviour, optical microscopy was performed on the fractured samples. After measuring the transverse crack density, it was concluded that the crack density in 90° ply was constant at the temperature range but different for the two cross ply laminates. It was nearly 0.545 (1/mm) for $[0_4/90_4]_s$ and 1.27 (1/mm) for $[0_2/90_2]_s$, however, as seen in Figure 15(a) and 15(b), it is evident that crack opening is much higher in $[0_4/90_4]_s$ than in $[0_2/90_2]_s$ laminates. The crack opening in cross ply laminates contributes to the stiffness reduction of transverse layers, thus transferring the load to the longitudinal layers, initiating splitting cracks and finally failure of the laminate. To better explain the function of observed 0° ply splitting cracks towards failure of $[0_2/90_2]_s$ and $[0_4/90_4]_s$ laminates, the failed specimens were cut width-wise and were mounted and polished as described previously. Optical microscopy revealed that there were more splitting cracks in $[0_2/90_2]_s$ compared to $[0_4/90_4]_s$ laminates, however the splitting cracks in $[0_4/90_4]_s$ are more influential since they initiated earlier due to the higher thickness of the transverse layers compared to $[0_2/90_2]_s$ laminates [29], and cause deeper cracks. These splitting cracks may grow along the specimen length when they are close to the specimen edges, resulting in a separated part which will fail due to fiber fracture. Therefore, in contrast to $[0_2/90_2]_s$ specimens, $[0_4/90_4]_s$ specimens fail in a non-localized manner via splitting cracks that cause load drop (see 16(b)) and, as a result, the strain to failure for $[0_4/90_4]_s$ specimens is lower than corresponding $[0_2/90_2]_s$ specimens (compare Figures 13 and 16).

Representative stress-strain curves for $[0_4/90_4]_s$ specimens at different temperatures are shown in Figure 16(a). As seen in the figure, analogous to $[0_2/90_2]_s$ specimens, the strain to failure decreases as the temperature increases except between 80 °C to 100 °C, where the strain increases slightly. This observation again corroborates the effect of temperature on weakening of the fiber-matrix interface in

longitudinal layers, which caused more splitting cracks at higher temperatures, and thus lower strains to failure. This failure behavior is very similar to the failure of $[0]_8$ specimens at different temperatures (see Figure 7).

Figure 14(b) illustrates Young's modulus versus temperature for $[0_4/90_4]_s$ specimens. As seen in the Figure, the trend in modulus degradation with temperature in $[0_4/90_4]_s$ specimens is analogous to that observed in $[0_2/90_2]_s$ specimens. Between 23 °C to 40 °C and between 40 °C to 50 °C there is, respectively, a 33.1% and 10.6 % decrease in Young's modulus. As a result, between 23 °C and 50 °C, $[0_4/90_4]_s$ specimens have 1.5 times higher decrease in Young's modulus than $[0_2/90_2]_s$ specimens which can be explained by twice higher thickness of 90 plies in $[0_4/90_4]_s$ laminate and higher effect of temperature on these plies.

The Young's modulus obtained using CLT was compared to that obtained at different temperatures in the experiments. At room temperature and 50 °C, the experimental modulus is 13.4 % and 24.2 % lower than the CLT modulus, respectively. At 80 °C and 100 °C the Young's modulus is constant based on CLT and is comparable with the results obtained in the experiments.

To explain the large difference between the experimental results and the CLT predictions at 50 °C , the behavior of $[0]_8$ and $[90]_8$ at higher temperatures must be considered. As the temperature increases to 50 °C, $[90]_8$ laminates show non-linear behavior and the strain to failure of these laminates increases from 0.4 % at room temperature to 0.47 % at 50 °C (see Figure 10) while the crack initiation for cross-ply laminates is 0.75 % due to the constraining effects of longitudinal layers on transverse layers [23]. It can be concluded that transverse layers show plastic deformation until 0.75 % strain, and thus computing the Young's modulus in $[0_2/90_2]_s$ and $[0_4/90_4]_s$ laminates based on the linear elastic modulus of $[90]_8$ laminates while these layers are in plastic region is not accurate. Indeed, the modulus evaluation near the glass transition temperature should be evaluated with more precise methods to account for non-linear effects.

4. Conclusions

The thermomechanical behavior of continuous E-glass/polyamide composites was investigated at various temperatures below and above the glass transition temperature, which was measured to be in the range of 63–67 °C with various characterization techniques. Thermomechanical quasi-static tensile tests were performed on $[0]_8$, $[90]_8$, $[0_2/90_2]_s$ and $[0_4/90_4]_s$ specimens using an environmental chamber mounted in a servo-hydraulic test frame, and fractography was utilized to study the underlying failure mechanisms. The $[0]_8$ and $[90]_8$ laminates exhibited three reduction stages in Young's modulus as a function of temperature, where the largest reduction was in the glass transition region and mainly attributed to matrix softening. At the glass transition region, the amorphous phase of the semi-crystalline polyamide matrix softens, and the ability of the matrix to transfer the load to the fibers decreased noticeably. The strength of $[0]_8$ and $[90]_8$ laminates nearly constantly decreased with increasing temperature to 80 °C as a result of weakening of the fiber-matrix bond, but decreases at a faster rate between 80 °C and 100 °C. This decrease was explained by large plastic deformation of polyamide matrix at 100 °C for $[90]_8$ laminates and large number of splitting cracks in $[0]_8$ laminates at 100 °C due to reduced interface strength between the glass fibers and the polyamide matrix. These findings were supported by SEM images and strain to failure measurements of laminates tested at different temperatures.

A different trend was observed for the $[0_2/90_2]_s$ and $[0_4/90_4]_s$ specimens, exhibiting the largest reduction in both strength and modulus before the glass transition temperature (i.e., up to 50 °C). This behavior was attributed to the degradation of transverse layers at temperatures near the glass transition temperature, as confirmed by SEM imaging, and the pronounced influence on the laminate degradation due to the thick transverse layers. Beyond 50 °C, the cross-ply laminates did not exhibit any strength or modulus degradation as a result of the constraining effects of the longitudinal layers on transverse layers, which mitigated further modulus degradation and delayed transverse cracking to higher strains, thus mitigating further strength degradation. This result is quite remarkable from a design perspective since, for the E-glass/polyamide cross-ply laminates studied, the strength and modulus degradation at

temperatures greater than T_g can be mitigated. In particular, for structural applications where exposure to elevated temperatures is unavoidable such as wind turbine blades, the use of a low cost high performance E-glass/polyamide laminate can provide a suitable replacement for more conventional glass/epoxy laminates.

In order to realize the replacement of glass/epoxy laminates with low cost recyclable glass/polyamide laminates, further complimentary studies are required. In particular, different laminate layups and stacking sequences should be investigated to better understand the influence of temperature on laminate strength and modulus degradation. The laminate strength and modulus degradation mitigation mechanisms at temperatures greater than the glass transition temperature, including ply softening and constraining effects which have an apparent temperature dependency, must be investigated for other laminates. Furthermore, the influence of temperature on the fatigue performance and progressive damage evolution must also be studied in order to understand the damage tolerability of continuous glass/epoxy laminates.

Acknowledgments

Tarbiat Modares University and the University of Waterloo are greatly acknowledged for funding in support of the study.

References

- [1] J.S. Lyons, Time and Temperature Effects on the Mechanical Properties of Glass-Filled Amide-Based Thermoplastics, *Polym. Test.* 17 (1998) 237–245.
- [2] X. Huang, J.W. Gillespie, R.F. Eduljee, Effect of temperature on the transverse cracking behavior of cross-ply composite laminates, *Compos. Part B Eng.* 28 (1997) 419–424.
- [3] B. Vieille, L. Taleb, About the influence of temperature and matrix ductility on the behavior of carbon woven-ply PPS or epoxy laminates: Notched and unnotched laminates, *Compos. Sci. Technol.* 71 (2011) 998–1007.

- [4] L. Sorrentino, D.S. de Vasconcellos, M. D'Auria, F. Sarasini, J. Tirillò, Effect of temperature on static and low velocity impact properties of thermoplastic composites, *Compos. Part B Eng.* 113 (2017) 100–110.
- [5] B. Antoun, A. Arzoumanidis, H.J. Qi, M. Silberstein, A. Amirkhizi, J. Furmanski, *Challenges in Mechanics of Time Dependent Materials*, Volume 2, 2017.
- [6] F. Rezaei, R. Yunus, N.A. Ibrahim, Effect of fiber length on thermomechanical properties of short carbon fiber reinforced polypropylene composites, *Mater. Des.* 30 (2009) 260–263.
- [7] D. Valentin, F. Paray, B. Guetta, The hygrothermal behaviour of glass fibre reinforced Pa66 composites: A study of the effect of water absorption on their mechanical properties, *J. Mater. Sci.* 22 (1987) 46–56.
- [8] X. Gabrion, V. Placet, F. Trivaudey, L. Boubakar, About the thermomechanical behaviour of a carbon fibre reinforced high-temperature thermoplastic composite, *Compos. Part B Eng.* 95 (2016) 386–394.
- [9] A.G. Gibson, M.E.O. Torres, T.N.A. Browne, S. Feih, A.P. Mouritz, High temperature and fire behaviour of continuous glass fibre/polypropylene laminates, *Compos. Part A Appl. Sci. Manuf.* 41 (2010) 1219–1231.
- [10] J.M.L. Reis, F.L. Chaves, H.S. Da Costa Mattos, Tensile behaviour of glass fibre reinforced polyurethane at different strain rates, *Mater. Des.* 49 (2013) 192–196.
- [11] B. Alcock, N.O. Cabrera, N.M. Barkoula, C.T. Reynolds, L.E. Govaert, T. Peijs, The effect of temperature and strain rate on the mechanical properties of highly oriented polypropylene tapes and all-polypropylene composites, *Compos. Sci. Technol.* 67 (2007) 2061–2070.
- [12] W. Hufenbach, M. Gude, R. Böhm, M. Zscheyge, The effect of temperature on mechanical properties and failure behaviour of hybrid yarn textile-reinforced thermoplastics, *Mater. Des.* 32 (2011) 4278–4288.
- [13] A. Malpot, F. Touchard, S. Bergamo, Effect of relative humidity on mechanical properties of a woven thermoplastic composite for automotive application, *Polym. Test.* 48 (2015) 160–168.
- [14] J.F. Mano, J.C. Viana, Effects of the strain rate and temperature in stress-strain tests: Study of the glass transition of a polyamide-6, *Polym. Test.* 20 (2001) 937–943.
- [15] A. Launay, Y. Marco, M.H. Maitournam, I. Raoult, Modelling the influence of temperature and relative humidity on the time-dependent mechanical behaviour of a short glass fibre reinforced polyamide, *Mech. Mater.* 56 (2013) 1–10.
- [16] Z. Wang, Y.X. Zhou, R.K. Mallick, Effects of temperature and strain rate on the tensile behavior of short fiber reinforced polyamide-6, *Polym. Compos.* 23 (2002) 858–871.
- [17] M. Eftekhari, A. Fatemi, Tensile behavior of thermoplastic composites including temperature, moisture, and hygrothermal effects, *Polym. Test.* 51 (2016) 151–164.
- [18] Rijswijk K.V. 2006. “Thermoplastic Composite Wind Turbine Blades,” Ph.D. thesis, Delft University of Technology, Delft.
- [19] A. Pegoretti, L. Fambri, C. Migliaresi, Interfacial stress transfer in nylon-6/E-Glass microcomposites: Effect of temperature and strain rate, *Polym. Compos.* 21 (2000) 466–475.
- [20] A. Pegoretti, M. Fidanza, C. Migliaresi, A.T. DiBenedetto, Toughness of the fiber/matrix interface in nylon-6/glass fiber composites, *Compos. Part A Appl. Sci. Manuf.* 29 (1998) 283–291.
- [21] M. Machado, U.D. Cakmak, I. Kallai, Z. Major, Thermomechanical viscoelastic analysis of woven-reinforced thermoplastic-matrix composites, *Compos. Struct.* 157 (2016) 256–264.
- [22] S. Ropers, M. Kardos, T.A. Osswald, A thermo-viscoelastic approach for the characterization and modeling of the bending behavior of thermoplastic composites, *Compos. Part A Appl. Sci. Manuf.* 90 (2016) 22–32.
- [23] M. Nikforooz, M. Golzar, M.M. Shokrieh, J. Montesano, Processability and performance of continuous glass fiber/polyamide laminates for structural load-bearing applications. *Compos. Part A Appl. Sci. Manuf.*, 105 (2018) 156–164.

- [24] M. Arhant, P.Y. Le Gac, M. Le Gall, C. Burtin, C. Briçon, P. Davies, Effect of sea water and humidity on the tensile and compressive properties of carbon-polyamide 6 laminates, *Compos. Part A Appl. Sci. Manuf.* 91 (2016) 250–261.
- [25] C.A. Mahieux, K.L. Reifsnider, Property modeling across transition temperatures in polymers: A robust stiffness - Temperature model, *Polymer (Guildf)*. 42 (2001) 3281–3291.
- [26] Y.S. Chang, J.J. Lesko, S.W. Case, D.A. Dillard, K.L. Reifsnider, The Effect of Fiber-Matrix Interphase Properties on the Quasi-Static Performance of Thermoplastic Composites, *J. Thermoplast. Compos. Mater.* 7 (1994) 311–324.
- [27] D.P.N. Vlasveld, S.G. Vaidya, H.E.N. Bersee, S.J. Picken, A comparison of the temperature dependence of the modulus, yield stress and ductility of nanocomposites based on high and low MW PA6 and PA66, *Polymer (Guildf)*. 46 (2005) 3452–3461.
- [28] R. Talreja, Assessment of the fundamentals of failure theories for composite materials, *Compos. Sci. Technol.* 105 (2014) 190–201.
- [29] J.E. Bailey, P.T. Curtis, A. Parvizi, On the Transverse Cracking and Longitudinal Splitting Behaviour of Glass and Carbon Fibre Reinforced Epoxy Cross Ply Laminates and the Effect of Poisson and Thermally Generated Strain, *Proc. R. Soc. A Math. Phys. Eng. Sci.* 366 (1979) 599–623.

Figures

Figure 1. Representation of thermomechanical quasi-static tensile test.

Figure 2. DSC thermogram of E-glass/polyamide prepreg.

Figure 3. DMA results for $[0_2/90_2]_s$ E-glass/polyamide laminates. a) E' and $\tan(\delta)$ versus temperature b) E'' versus temperature.

Figure 4. Linear coefficient of thermal expansion versus temperature from the TMA test.

Figure 5. a) Tensile strength and b) Young's modulus versus temperature for $[0]_8$ specimens.

Figure 6. SEM images of fractured surfaces tested at a) 23°C, b) 50 °C and c) 80 °C for $[0]_8$ laminates.

Figure 7. a) Quasi-static tensile stress-strain curves for $[0]_8$ specimens tested at different temperatures b) $[0]_8$ failed specimens in thermomechanical quasi-static tensile loading c) splitting cracks.

Figure 8. a) Tensile strength and b) Young's modulus versus temperature for $[90]_8$ specimens.

Figure 9. SEM images of fracture surfaces tested at a) 23°C, b) 50 °C and c) 80 °C d) 100 °C for $[90]_8$ laminates.

Figure 10. a) Stress-strain curves for $[90]_8$ specimens tested at different temperatures b) Specimen failure at 100 °C.

Figure 11. Tensile strength and Young's modulus versus temperature for $[0_2/90_2]_s$ specimens.

Figure 12. SEM images of fractured surfaces of $[0_2/90_2]_s$ laminates tested at a) 23°C, b) 40 °C, c) 50 °C and d) 80 °C.

Figure 13. a) Stress-strain curves for $[0_2/90_2]_s$ specimens tested at different temperatures b) Failed $[0_2/90_2]_s$ specimens.

Figure 14. a) Tensile strength and b) Young's modulus versus temperature for $[0_4/90_4]_s$ specimens.

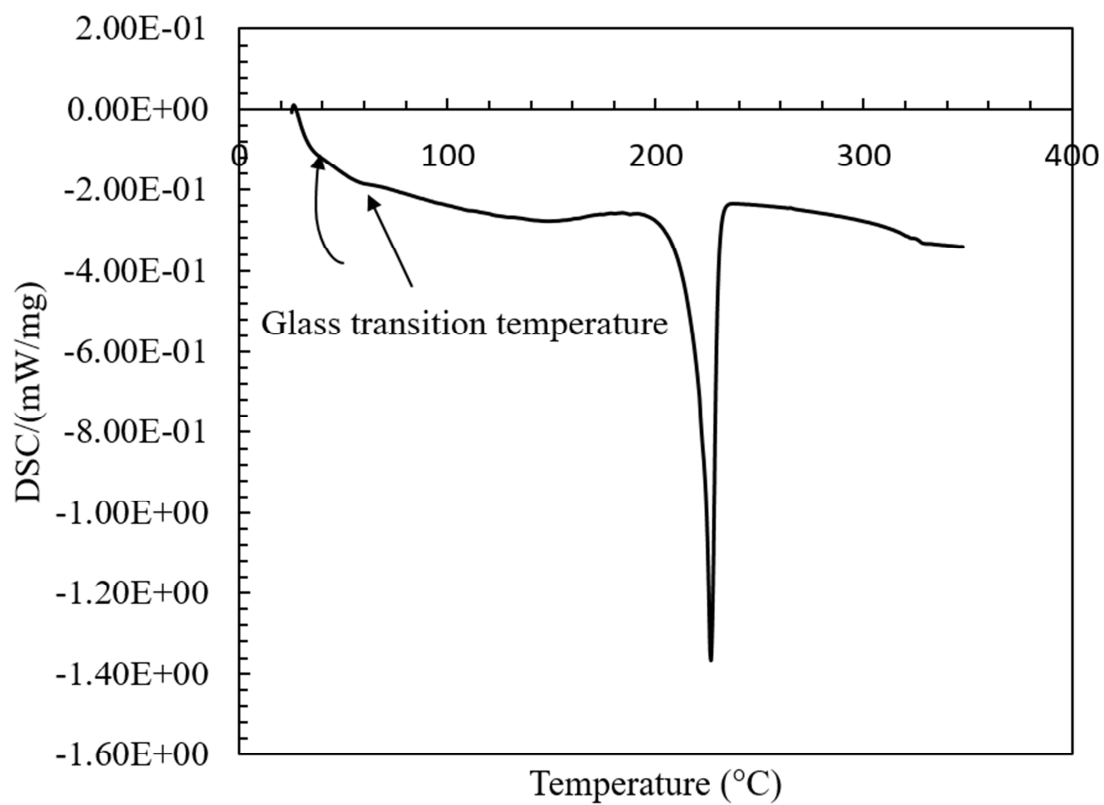
Figure 15. Transverse cracking and longitudinal splitting in $[0_2/90_2]_s$ and $[0_4/90_4]_s$ laminates. a) Transverse cracking in $[0_2/90_2]_s$ laminates b) Transverse cracking in $[0_4/90_4]_s$ laminates c) longitudinal splitting in $[0_2/90_2]_s$ laminates d) longitudinal splitting in $[0_4/90_4]_s$ laminates.

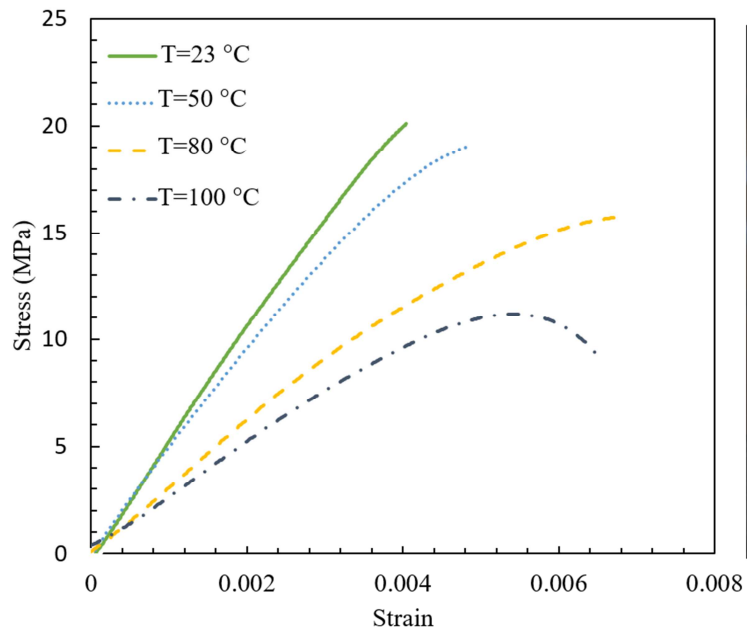
Figure 16. a) Stress-strain curves for $[0_4/90_4]_s$ specimens at different temperatures b) Failed $[0_4/90_4]_s$ specimens.

Tables

Table 1. Dimensions of the specimens used for quasi-static tensile tests.

Lamination	L_1	L_2	W_1	T_1	T_2
$[0]_8$	110	20	15	1.4 ± 0.1	1
$[90]_8$	110	20	15, 20	1.4 ± 0.1	1
$[0_2/90_2]_s$	110	20	15	1.4 ± 0.1	1
$[0_4/90_4]_s$	110	20	15	2.9 ± 0.1	1.5



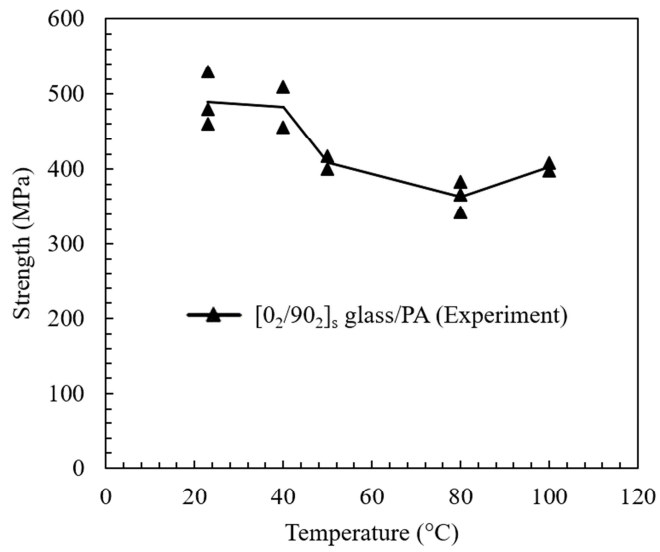


a)

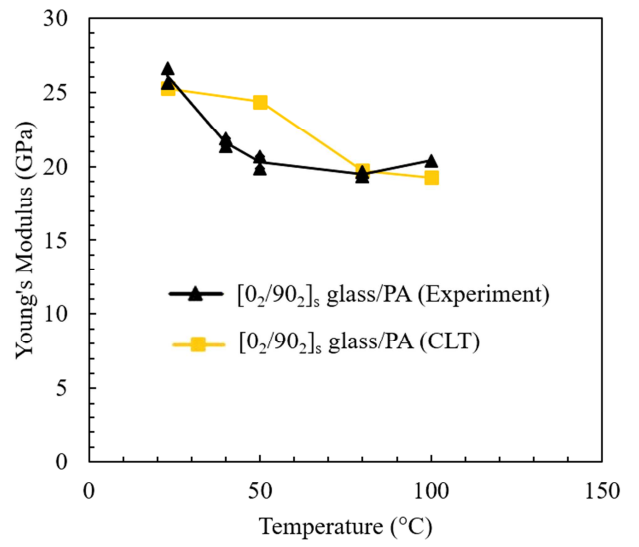


b)

ACCEPTED MANUSCRIPT



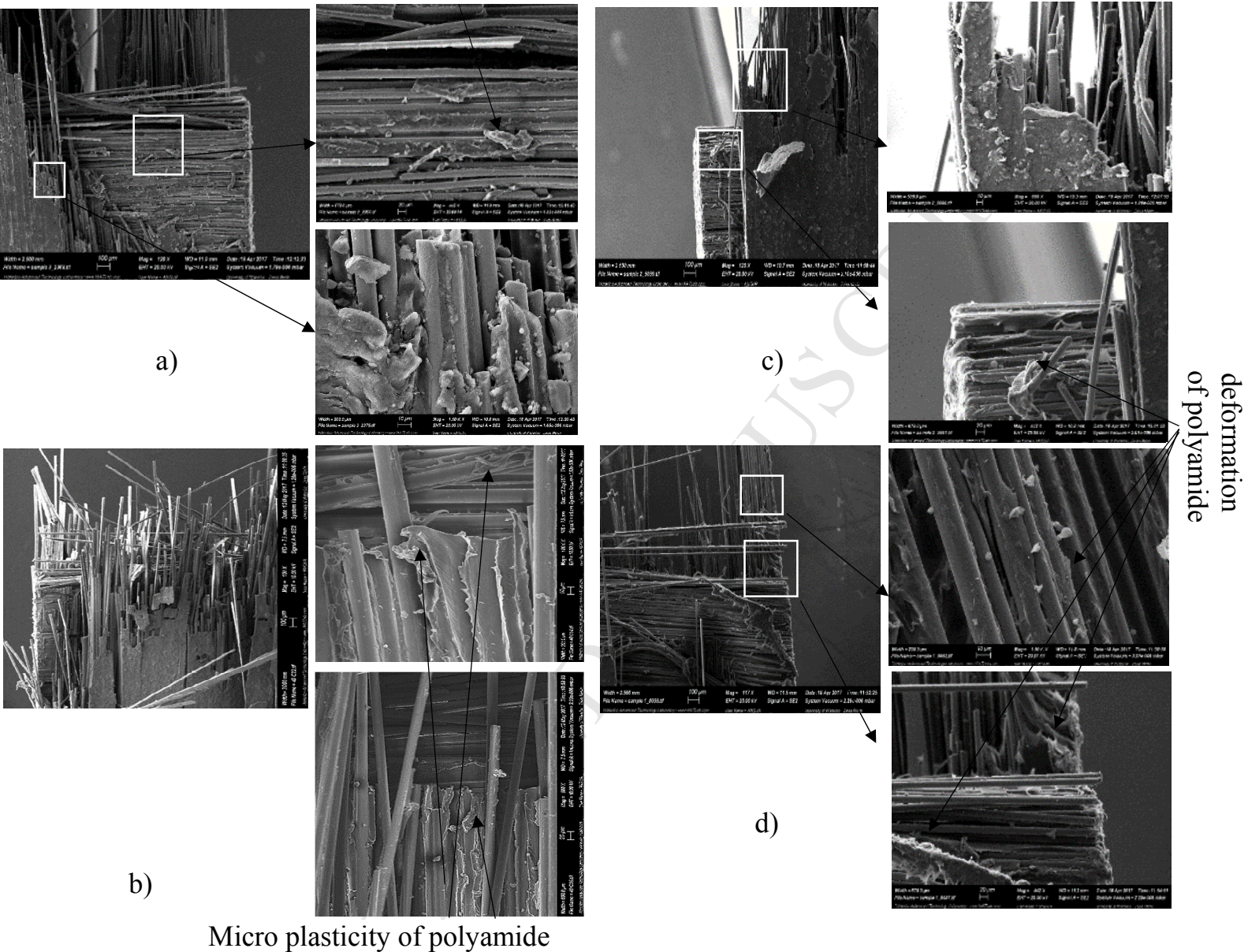
a)



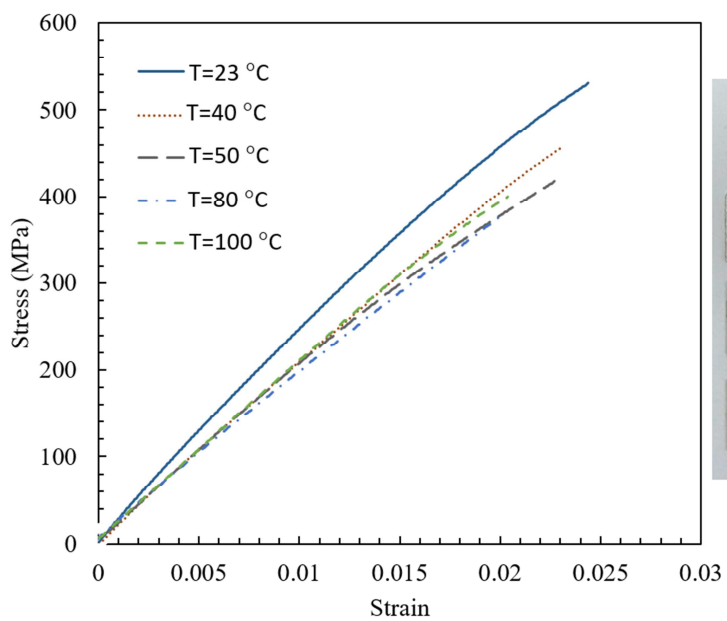
b)

ACCEPTED MANUSCRIPT

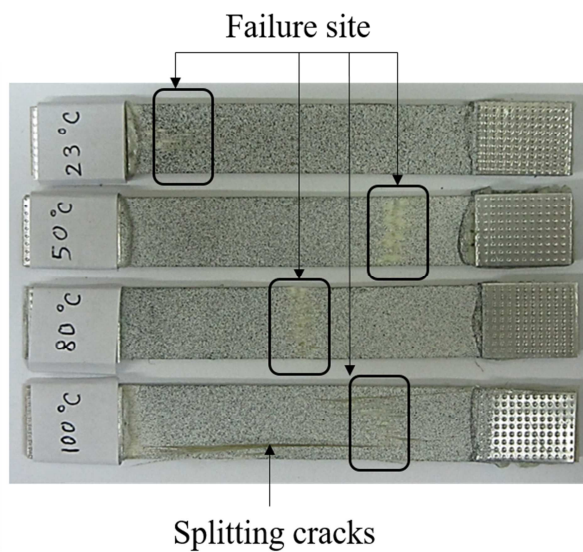
Chunk of polyamide

deformation
of polyamide

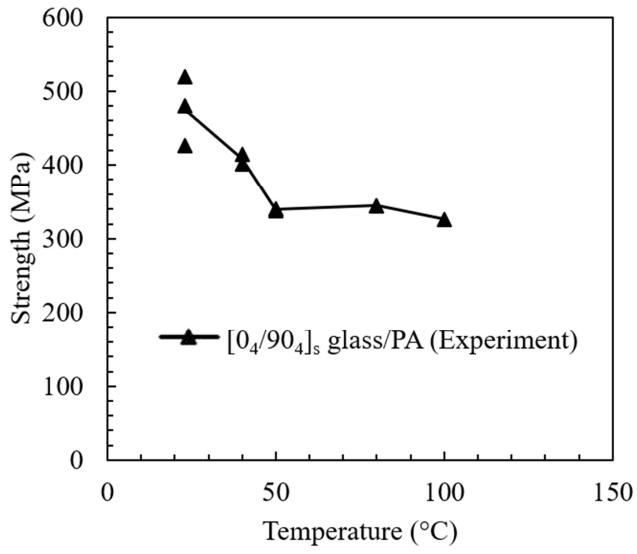
Micro plasticity of polyamide



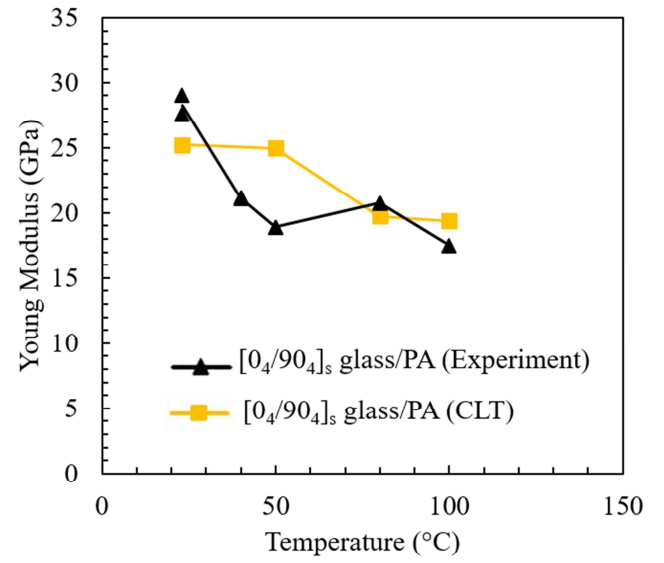
a)



b)

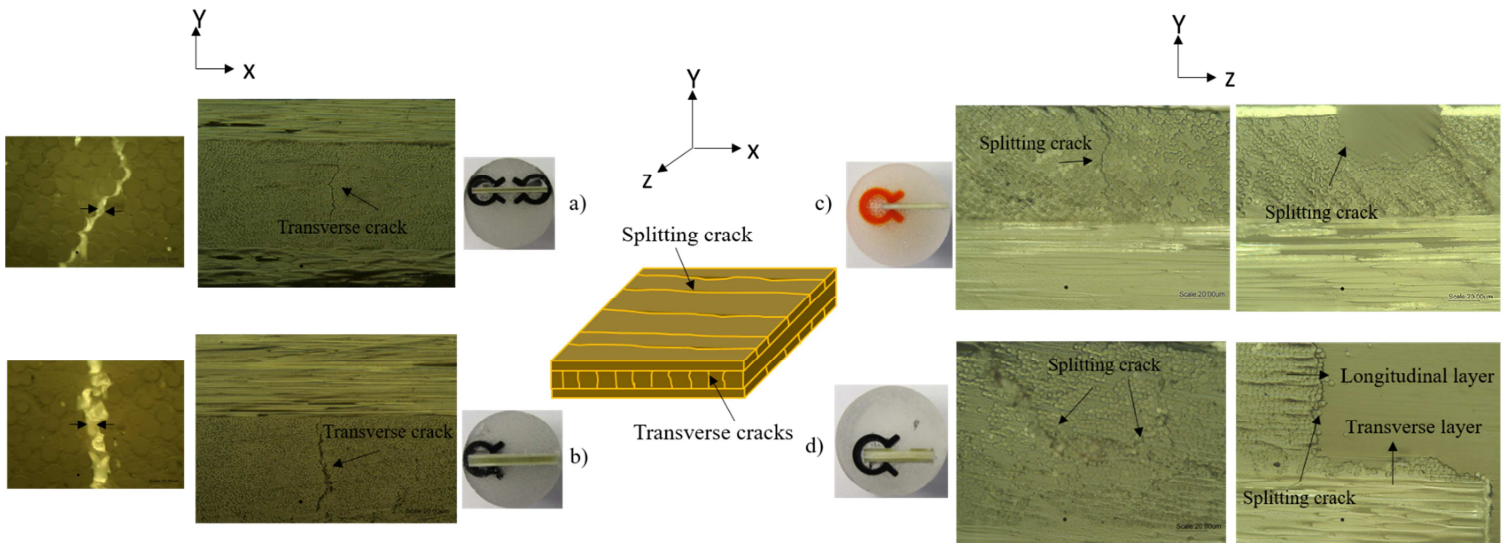


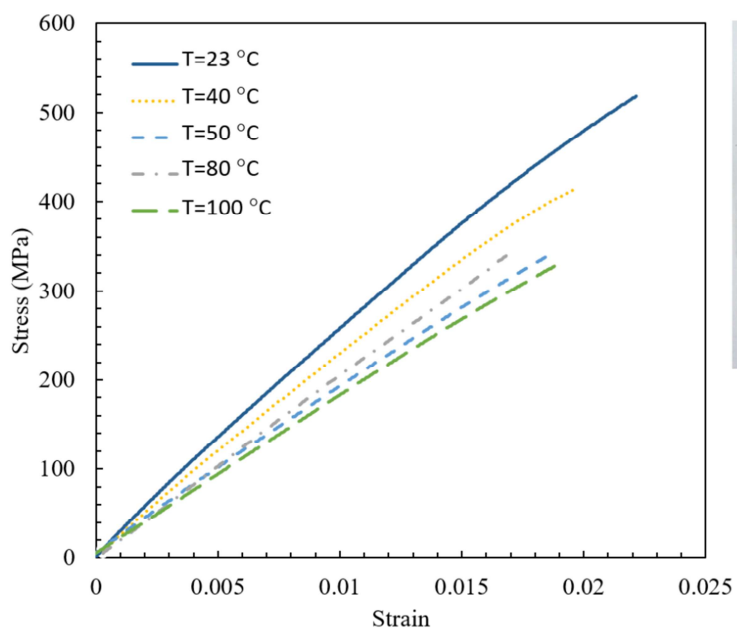
a)



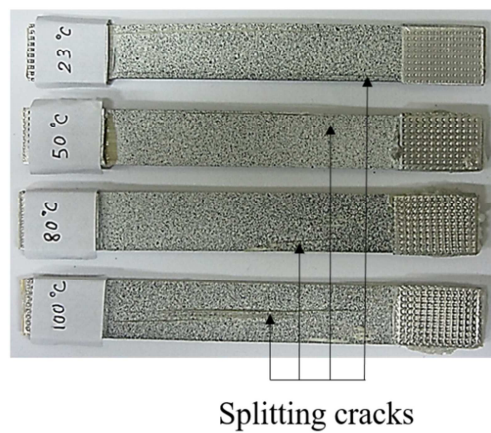
b)

ACCEPTED MA



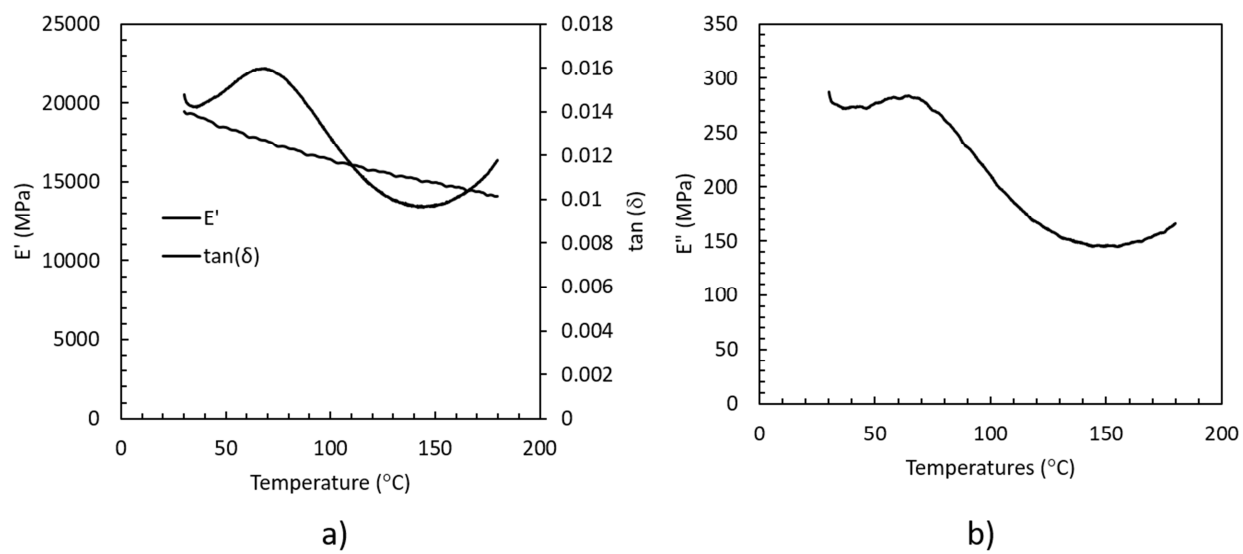


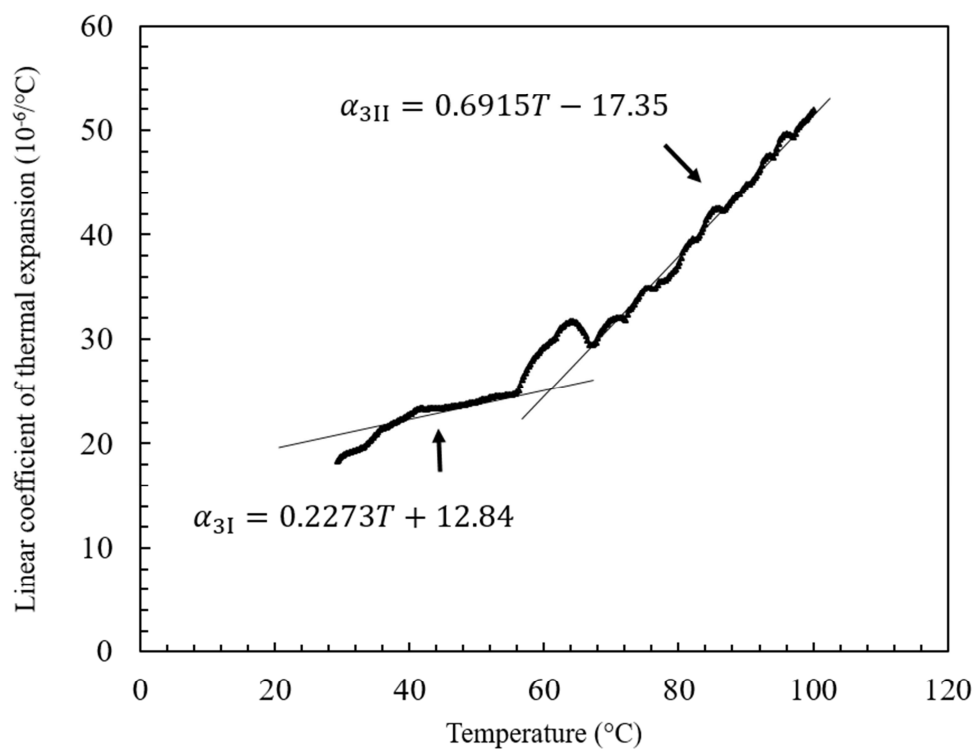
a)

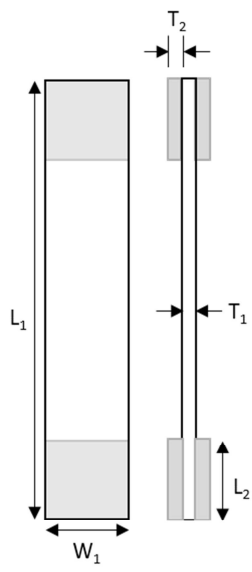


b)

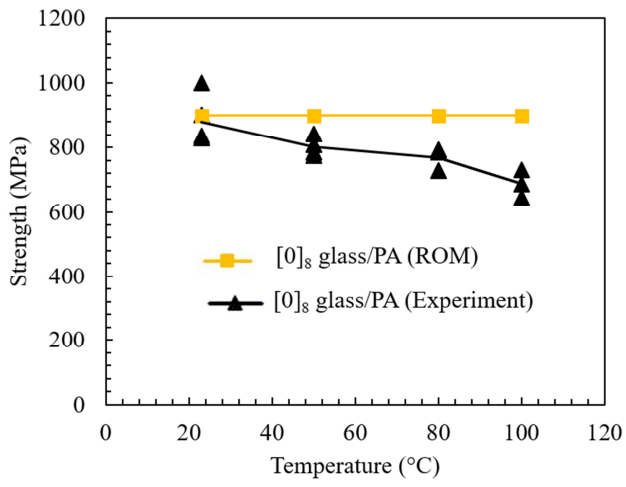
ACCEPTED MANUSCRIPT



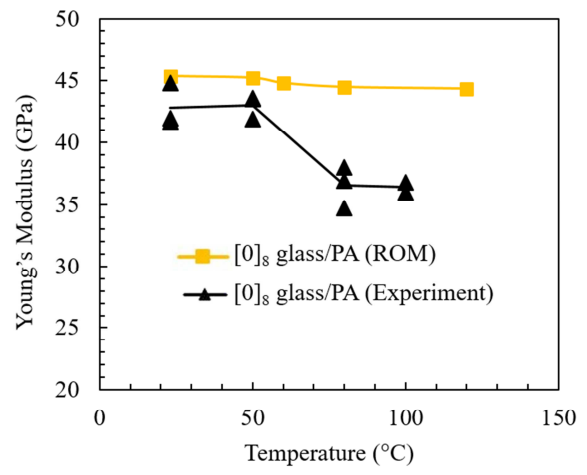




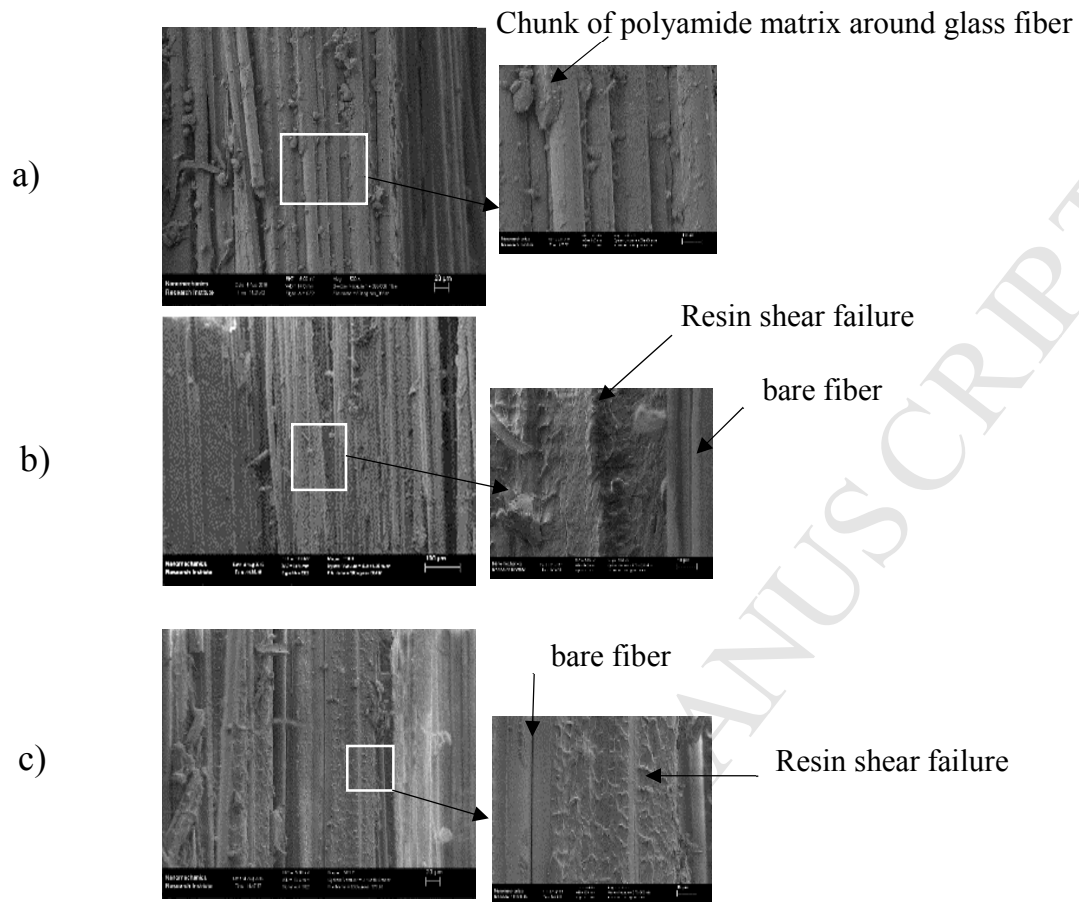
ACCEPTED MANUSCRIPT

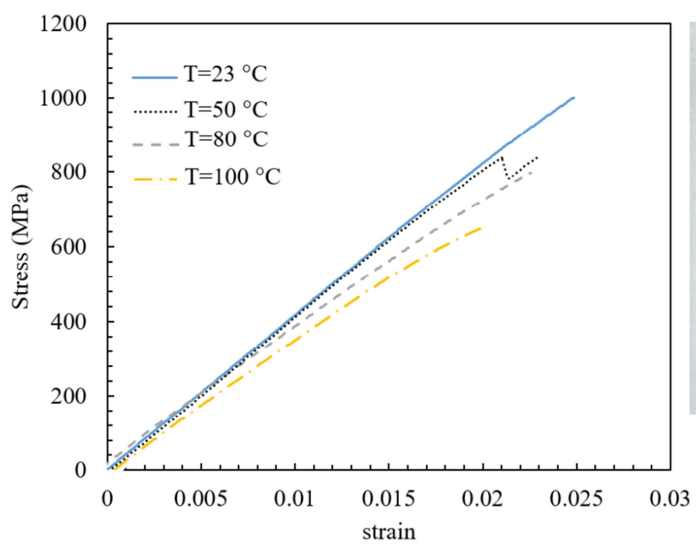


a)

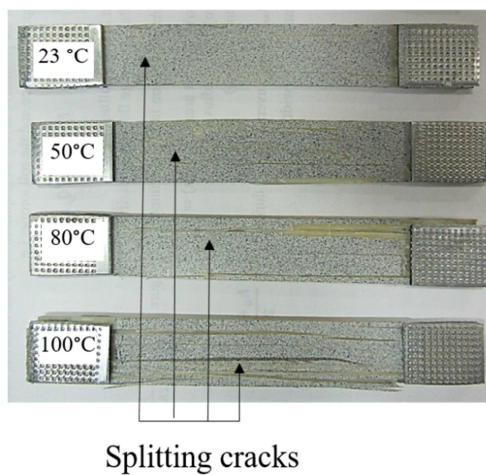


b)



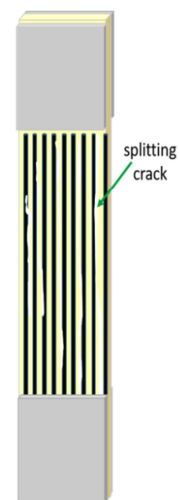


a)

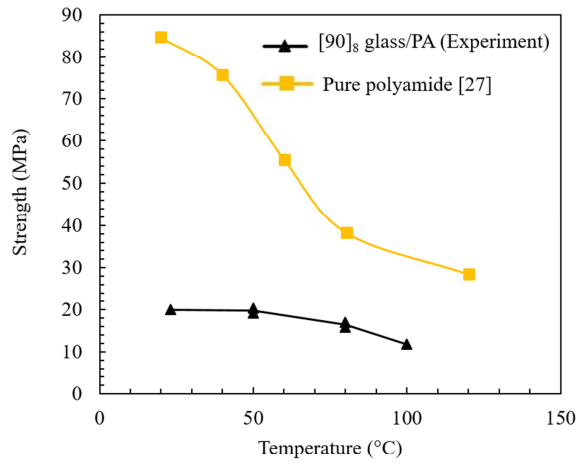


Splitting cracks

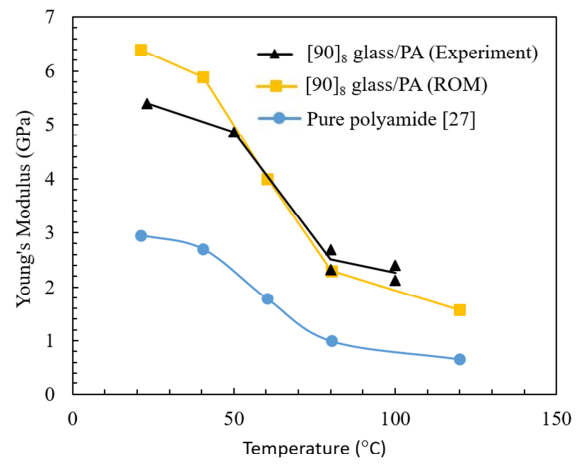
b)



c)

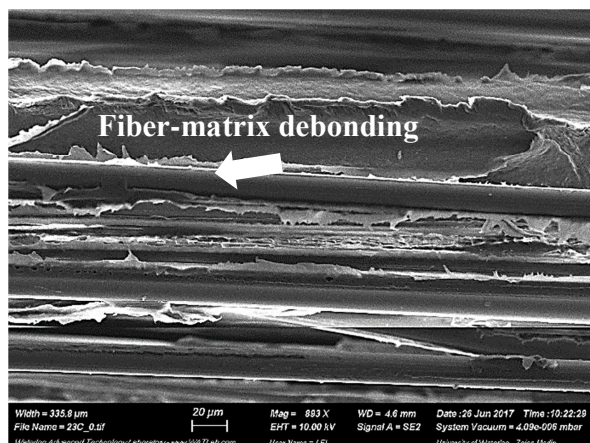


a)

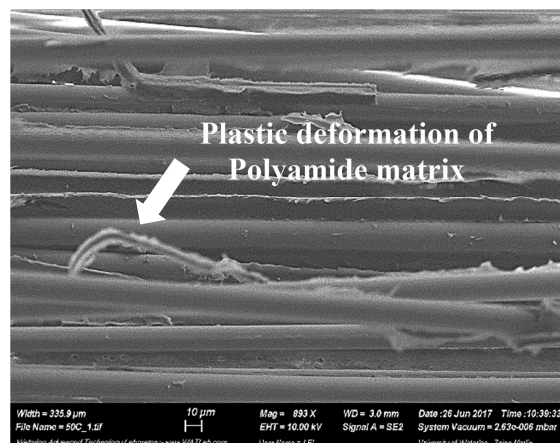


b)

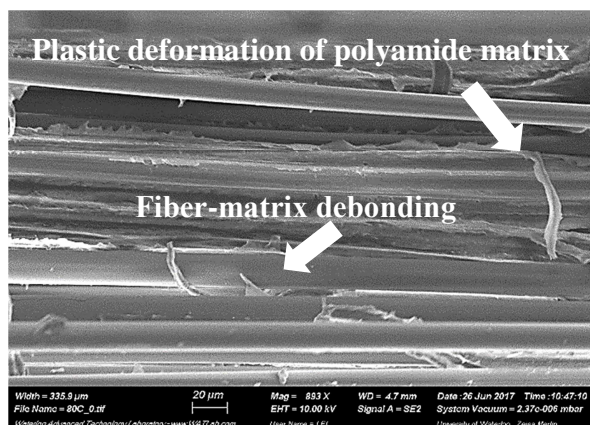
ACCEPTED MANUSCRIPT



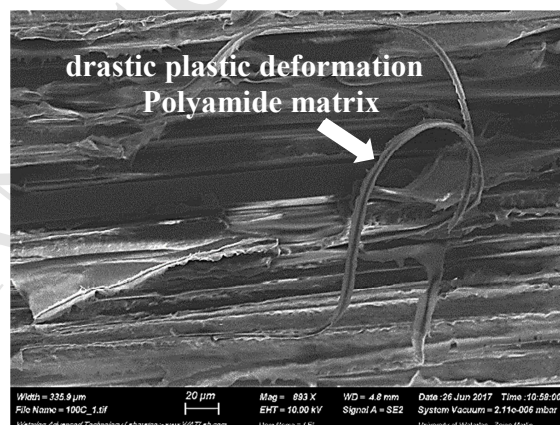
a)



b)



c)



d)

Highlights

- The thermomechanical behavior of continuous E-glass/polyamide composites was investigated in lamina and laminate level.
- Glass transition temperature of the material was measured with DSC, TMA and DMA.
- $[0]_8$ and $[90]_8$ laminates displayed three reduction stages in modulus versus temperature, where the largest reduction was in the glass transition region.
- $[0_2/90_2]_s$ and $[0_4/90_4]_s$ laminates displayed the largest modulus reduction prior to the glass transition temperature.
- Effects of temperature on material failure were investigated using optical and scanning electron microscopy.